Probabilistic Margins for Instance Reweighting in Adversarial Training

Qizhou Wang[1,*], **Feng Liu**[2,*], **Bo Han**[1,†], **Tongliang Liu**[3], **Chen Gong**[4,5],
Gang Niu[6], **Mingyuan Zhou**[7], **Masashi Sugiyama**[6,8]
[1]Department of Computer Science, Hong Kong Baptist University
[2]DeSI Lab, Australian Artificial Intelligence Institute, University of Technology Sydney
[3]TML Lab, School of Computer Science, Faculty of Engineering, The University of Sydney
[4]PCA Lab, Key Lab of Intelligent Perception and Systems for High-Dimensional Information of MoE
[5]Jiangsu Key Lab of Image and Video Understanding for Social Security,
School of Computer Science and Engineering, Nanjing University of Science and Technology
[6]RIKEN Center for Advanced Intelligence Project (AIP)
[7]McCombs School of Business, The University of Texas at Austin
[8]Graduate School of Frontier Sciences, The University of Tokyo
{csqzwang, bhanml}@comp.hkbu.edu.hk, feng.liu@uts.edu.au,
tongliang.liu@sydney.edu.au, chen.gong@njust.edu.cn, gang.niu.ml@gmail.com
mingyuan.zhou@mccombs.utexas.edu, sugi@k.u-tokyo.ac.jp

Abstract

Reweighting adversarial data during training has been recently shown to improve adversarial robustness, where data *closer* to the current decision boundaries are regarded as *more critical* and given *larger weights*. However, existing methods measuring the closeness are not very reliable: they are *discrete* and can take only a few values, and they are *path-dependent*, i.e., they may change given the same start and end points with different attack paths. In this paper, we propose three types of *probabilistic margin* (PM), which are *continuous* and *path-independent*, for measuring the aforementioned closeness and reweighting adversarial data. Specifically, a PM is defined as the difference between two *estimated class-posterior probabilities*, e.g., such a probability of the true label minus the probability of the most confusing label given some natural data. Though different PMs capture different *geometric properties*, all three PMs share a negative correlation with the vulnerability of data: data with larger/smaller PMs are safer/riskier and should have smaller/larger weights. Experiments demonstrated that PMs are reliable and PM-based reweighting methods outperformed state-of-the-art counterparts.

1 Introduction

Deep neural networks are susceptible to adversarial examples that are generated by changing natural inputs with malicious perturbation [17, 20, 37, 39]. Those examples are imperceptible to human eyes but can fool deep models to make wrong predictions with high confidence [3, 35]. As deep learning has been deployed in many real-life scenarios and even safety-critical systems [15, 16, 28], it is crucial to make such deep models reliable and safe [19, 25, 30]. To obtain more reliable deep models, *adversarial training* (AT) [2, 10, 29] was proposed as one of the most effective methodologies against adversary attacks (i.e., maliciously changing natural inputs). Specifically, during training, it simulates adversarial examples (e.g., via *project gradient descent* (PGD) [1, 29, 46, 41]) and train a classifier

[*] Equal contribution.

[†] Corresponding author.

35th Conference on Neural Information Processing Systems (NeurIPS 2021).

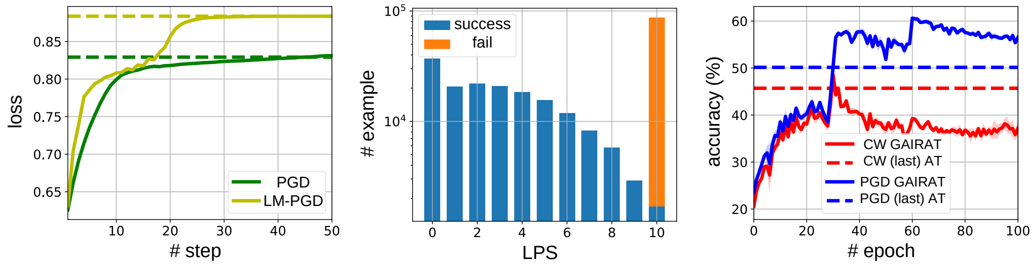

(a) Loss Curve (b) Histogram (c) Accuracy Curve

Figure 1: An illustration for the drawbacks of LPS. (a) suggested that LPS is path-dependent and the PGD method (PGD) may get stuck at sub-optimal points. Here, we proved the existence of a better (not optimal) solution given by a LM-PGD method (Appendix A). LPSs are 50 and 14 estimated by PGD and LM-PGD, respectively, which reveals that LPS depends on the adopted attacks. (b) suggested that LPS can take only a few discrete values, and it may have confusing meanings when LPS met its maximum. In this case, one can hardly distinguish non-robust data with LPS being 10 and safe data that are insensitive to be attacked. (c) showed that the accuracy of GAIRAT (on *CIFAR-10*) dropped when facing CW attacks. The main reason is that LPS is not reliable in measuring the distance, and thus it makes wrong judgments when assigning weights for non-robust instances.

with the simulated adversarial examples [29, 46]. Since such a model has seen some adversarial examples during its training process, it can defend against certain adversarial attacks and is more *adversarial-robust* than traditional classifiers trained with natural data [7, 14, 36, 49].

Recently, researchers have found that over-parameterized deep networks still have the insufficient model capacity, due to the overwhelming smoothing effect of AT [47, 33]. As a result, they proposed *instance-reweighted adversarial training*, where adversarial data should have unequal importance given limited model capacity [47]. Concretely, they suggested that data *closer* to the decision boundaries are much more vulnerable to be attacked [45, 47] and should be assigned larger weights during training. To characterize these *geometric properties* of data (i.e., the closeness between the data and decision boundaries), Zhang et al. [47] suggested an estimation in the input space, i.e., the *least PGD steps* (LPS), to identify non-robust (i.e., easily-be-attacked) data. Specifically, LPS is the number of steps to make the adversarial variant of such an instance cross the decision boundaries, starting from a natural instance. Based on LPS, they achieved state-of-the-art performance via a general framework termed *geometry-aware instance-reweighted adversarial training* (GAIRAT).

However, existing methods [18, 22, 38] in measuring the geometric properties of data are *path-dependent*, i.e., they may change even given the same start (a natural example) and end point (the adversarial variant); and they are *discrete* with only a few valid values (Figure 2). The path-dependency makes the computation unstable, where the results may change given different attack paths. The discreteness makes the measurement ambiguous since each value would have several (even contradictory) meanings. We take LPS as an example to demonstrate a path-dependent (Figure 1a) and discrete measurement (Figure 1b). As we can see in Figure 1c, the consequence is non-negligible: although adopting LPS (i.e., GAIRAT) reveals improvement for the PGD-100 attack [29], its performance is well below AT regarding the CW attack [9].

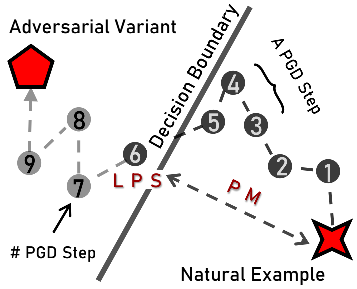

Figure 2: LPS and the proposed PM in comparison. The PGD method takes 6 step to find an instance to violate the decision boundary (i.e., LPS equals 6), while PM is continuous to represent this distance.

In this paper, we propose the *probabilistic margin* (PM), which is *continuous* and *path-independent*, for reweighting adversarial data during AT. PM is a geometric measurement from a data point to the closest decision boundary, following the *multi-class margin* [23] in traditional geometry-aware machine learning. Note that, instead of choosing the input space as LPS, PM is defined by the *estimated class-posterior probabilities* from the model outputs, e.g., such the probability of the true label minus the probability of the most confusing label given some natural data. Therefore, PM is computed in a low-dimensional embedding space with normalization, alleviating the troubles in comparing data from different classes.

The definition of PM is general, where we consider three specifications, namely, $\texttt{PM}^{\text{nat}}$, $\texttt{PM}^{\text{adv}}$, and $\texttt{PM}^{\text{dif}}$. Concretely, $\texttt{PM}^{\text{nat}}$ and $\texttt{PM}^{\text{adv}}$ are the PM scores regarding natural and adversarial data, respectively. They assume that the vulnerability of data is revealed by the closeness regarding either the natural data or the adversarial variants. However, the definition of $\texttt{PM}^{\text{dif}}$ is slightly different, which is the distance of a natural data point to its adversarial variant. $\texttt{PM}^{\text{dif}}$ is viewed as a conceptual counterpart of LPS, but is critically different since it is continuous and path-independent. In our paper, we verified the effectiveness of $\texttt{PM}^{\text{nat}}$ and $\texttt{PM}^{\text{adv}}$ and showed that they can represent the geometric properties of data well. Note that, though these types of PMs depict different geometric properties, they all share a negative correlation with the vulnerability of data—larger/smaller PMs indicate that the corresponding data are safer/riskier and thus should be assigned with smaller/larger weights.

Eventually, PM is employed for reweighting adversarial data during AT, where we propose the *Margin-Aware Instance reweighting Learning* (MAIL). With a non-increased weight assignment function in Eq. (8), MAIL pays much attention to those non-robust data. In experiments, MAIL was combined with various forms of commonly-used AT methods, including traditional AT [29], MART [40], and TRADES [45]. We demonstrated that PM is more reliable than previous works in geometric measurement, irrelevant to the forms of the adopted objectives. Moreover, in comparison with advanced methods, MAIL revealed its state-of-the-art performance against various attack methods, which benefits from our path-independent and continuous measurement.

2 Preliminary

2.1 Traditional Adversarial Training

For a K-classification problem, we consider a training dataset $S = \{(x_i, y_i)\}_{i=1}^n$ independently drawn from a distribution $\mathcal{D}$ and a deep neural network $h(x; \theta)$ parameterized by θ. This deep classifier $h(x; \theta)$ predicts the label of an input data via $h(x; \theta) = \arg\max_k \mathbf{p}_k(x; \theta)$, with $\mathbf{p}_k(x, \theta)$ being the predicted probability (softmax on logits) for the k-th class.

The goal of AT is to train a model with a low adversarial risk regarding the distribution $\mathcal{D}$, i.e., $\mathcal{R}(\theta) = \mathbb{E}_{(x,y)\sim\mathcal{D}}\left[\max_{\delta\in\Delta} \ell(x + \delta, y; \theta)\right]$, where Δ is the threat model, defined by an L_p-norm bounded perturbation with the radius ϵ: $\Delta = \{\delta \in \mathbb{R}^d \mid ||\delta||_p \leq \epsilon\}$. Therein, AT computes the new perturbation to update the model parameters, where the PGD method [29] is commonly adopted: for a (natural) example x_i, it starts with random noise ξ and repeatedly computes

$$\delta_i^{(t)} \leftarrow \texttt{Proj}\left[\delta_i^{(t-1)} + \alpha \texttt{sign}\left(\nabla_\theta \ell(x_i + \delta_i^{(t-1)}, y_i; \theta)\right)\right], \tag{1}$$

with $\texttt{Proj}$ the clipping operation such that $\delta^{(t)}$ is always in Δ and $\texttt{sign}$ the signum function. Due to the non-convexity, we typically approximate the optimal solution by $\delta_i^{(T)}$ with T being the maximally allowed iterations. Accordingly, $\delta_i^{(T)}$ is viewed as the perturbation for the *most* adversarial example [47], and the learning objective function is formulated by

$$\arg\min_\theta \sum_i \ell(x_i + \delta_i^{(T)}, y_i; \theta). \tag{2}$$

Intuitively, AT corresponds to the *worst-case robust optimization*, continuously augmenting the training dataset with adversarial variants that highly confuse the current model. Therefore, it is a practical learning framework to alleviate the impact of adversarial attacks. Unfortunately, it leads to insufficient network capacity, resulting in unsatisfactory model performance regarding adversarial robustness. The reason is that, AT has an overwhelming smoothing effect in fitting highly adversarial examples [45], and thus consumes large model capacity to learn from some individual data points.

2.2 Geometry-Aware Adversarial Training

Zhang et al. [47] claimed that training examples should have unequal significance in AT, and proposed the *geometry-aware instance-reweighted adversarial training* (GAIRAT). It is a general framework to reweight adversarial data during training, where Eq. (2) is modified as

$$\arg\min_{\theta} \sum_i \omega_i \ell(x_i + \delta_i^{(T)}, y_i; \theta) \quad \text{s.t. } \omega_i \geq 0 \text{ and } \sum_i \omega_i = 1. \tag{3}$$

Note that, the constraints are required since the risk after weighting is consistent with the original one without weighting. Further, the generation of perturbation still follows Eq. (1). They revealed that data near decision boundary are much vulnerable to be attacked and require large weights.

LPS as a geometric measurement. In assigning weights, GAIRAT needs a proper measurement for the distance to the decision boundaries. They suggested the estimation in high-dimensional input space via LPS (Fig. 2), which is the least PGD iterations for a perturbation that leads to a wrong prediction. Intuitively, a small LPS indicates that the data point can quickly cross the decision boundary and thus close to it.

The drawbacks of LPS. Although promising results have been verified in experiments, LPS is path-dependent and limited by a few discrete values, where the consequence is non-negligible. In Figure 1(a), we showed that the PGD method will get stuck. Therefore, using LPS as a geometric measurement, we might identify non-robust examples as robust ones. Here, we modified the vanilla PGD method with the *line-searched* learning rate [43] and *Nesterov momentum* [31] (see Appendix A), termed *Line-search & Momentum-PGD* (LM-PGD), and we compared the loss curve of PGD with that of LM-PGD on one example. The maximal iterations of PGD was 50. As we can see, PGD almost converged at the 14-th step, and the loss value did not ascend anymore. As a result, LPS of this example was 50, and this example was taken as a robust one in the view of LPS. However, LM-PGD still ascended after the 14-th step and successfully attacked the instance at the 15-th step. This result means that such an instance is *not* a robust one, but LPS made a wrong judgment in its robustness. The main reason is that, LPS is heavily dependent on attack paths, even though both paths are highly similar.

Now, we demonstrate that the limited range of LPS would cause problems as well. In Figure 1b, we show the histogram of LPSs for data on CIFAR-10 [24]. Higher LPS values mean that these examples were more robust and required smaller weights during AT. It could be seen that LPS has a confusing meaning when it equaled the maximal value, which is 10 following [29]. For data whose LPSs were 10, they would be the most robust/safe ones. However, it could be seen that they still contained the critical data points (the blue part). Although the proportion of the critical data seems low, ignoring them during AT (i.e., assigning small weights for them) will cause problems. For example, the trained classifier's accuracy will drop significantly when facing the CW attack [9] (Figure 1c).

3 Probabilistic Margins for Instance Reweighting

The drawbacks of LPS motivate us to improve the measurement in discerning robust data and risky data, and we introduce our proposal in this section.

3.1 Geometry Information in view of Probabilistic Margin

Instead of using the input space as LPS, we suggest the measurement on estimated class-posterior probabilities, which are normalized embedding features (softmax on logits) in the range $[0, 1]$ for each dimension. Note that, without normalization, average distances from different classes might be of diverse scales (e.g., the average distance is 10 for the i-th class and 100 for the j-th class), increasing the challenge in comparing data from different classes (see Appendix B).

Inspired by the *multi-class margin* in margin theory [23], we propose the *probabilistic margin* (PM) regarding model outputs, namely,

$$\texttt{PM}(x, y; \theta) = \mathbf{p}_y(x; \theta) - \max_{j, j \neq y} \mathbf{p}_j(x; \theta), \tag{4}$$

where the first term in the r.h.s. is the *closeness* of x to the "center" of the true label y and the second term is the closeness to the nearest class except y (i.e., the most confusing label). The difference between the two terms is clearly a valid measurement, where the magnitude reflects the distance from the nearest boundary, and the signum indicates which side the data point belongs to. Figure 3

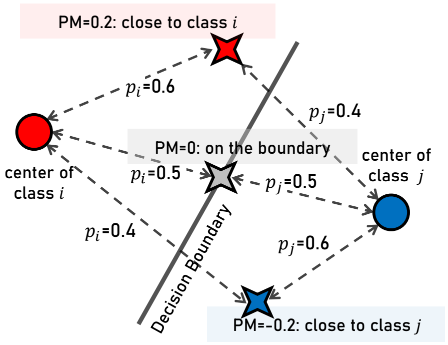

Figure 3: An illustration of PM, where p_i is the probability that a data point belongs to the i-th class. As a special example, here we assume $\mathtt{PM} = p_i - p_j$ with i the target y and j the nearest class except y.

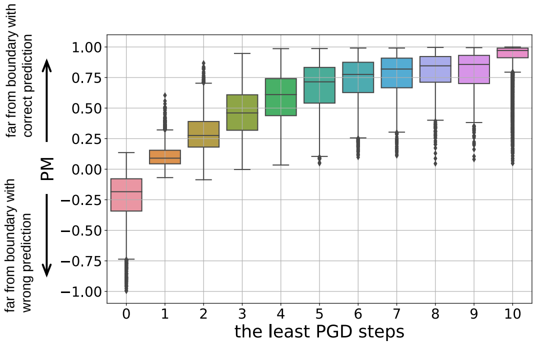

Figure 4: Comparison of LPS and PM ($\mathtt{PM}^{\text{nat}}$). An interquartile range box represents the middle 50% of the considered data with the inside line being the median; a whisker is the range for the bottom/top 5% data, and points above/below whiskers are outliers.

summarizes the key concepts, with i for the true label y and j for the most confusing class. For example, when $\mathbf{p}_y(x;\theta) = \mathbf{p}_j(x;\theta) = 0.5$, PM is 0 and the data point x is on the decision boundary between two classes; when $\mathbf{p}_y(x;\theta) = 0.6$ and $\mathbf{p}_j(x;\theta) = 0.4$, PM is positive and the data point x is much closer to the true label; if $\mathbf{p}_y(x;\theta) = 0.4$ and $\mathbf{p}_j(x;\theta) = 0.6$, PM is negative and the data point x is much closer to the most confusing class.

The above discussion indicates that PM can point out which geometric area a data point belongs to, where we discuss the following three scenarios: the *safe area* with large positive PMs, the *class-boundary-around data* with positive PMs close to 0, and the *wrong-prediction area* with negative PMs. The safe area contains guarded data that are insensitive to perturbation, which are safe and require low attention in AT (i.e., small weights); for the class-boundary-around data, they are much vulnerable to be attacked [45, 47] and thus need larger weights than the safe data; for data in the wrong-prediction area, they are the most critical since the attack method can successfully fool the current model, and thus they should be assigned the largest weights. For a data point, this indicates a negative correlation of its PM with the vulnerability, where a larger PM indicates a smaller weight is required for this data point. In realization, the measurement of PM can be employed for adversarial data or natural ones, which are of the forms:

$$\mathtt{PM}_i^{\text{adv}} = \mathbf{p}_{y_i}(x_i + \delta_i^{(T)};\theta) - \max_{j, j \neq y_i} \mathbf{p}_j(x_i + \delta_i^{(T)};\theta), \tag{5}$$

$$\mathtt{PM}_i^{\text{nat}} = \mathbf{p}_{y_i}(x_i;\theta) - \max_{j, j \neq y_i} \mathbf{p}_j(x_i;\theta), \tag{6}$$

for a data point x_i respectively. They assume that the vulnerability of data is revealed by the closeness regarding either the natural data or their adversarial variants. Besides these two basic cases, one can also consider the difference between the natural and adversarial predictions, namely,

$$\mathtt{PM}_i^{\text{dif}} = \mathbf{p}_{y_i}(x_i;\theta) - \mathbf{p}_{y_i}(x_i + \delta_i^{(t_i)};\theta), \tag{7}$$

where $t_i \leq T$ denotes LPS of x_i. $\mathtt{PM}^{\text{dif}}$ is a conceptual counterpart of LPS, while Eq. (7) is actually path-independent and continuous, which is more reliable than LPS. Note that, the valid range of $\mathtt{PM}^{\text{dif}}$ (i.e., $[0, 1]$) is different from that of $\mathtt{PM}^{\text{adv}}$ and $\mathtt{PM}^{\text{nat}}$ (i.e., $[-1, 1]$), which may bring unnecessary troubles since the geometric meanings of $\mathtt{PM}^{\text{nat}}$ and $\mathtt{PM}^{\text{dif}}$ are highly similar. Therefore, in our experiments, we mainly verify the effectiveness of $\mathtt{PM}^{\text{adv}}$ and $\mathtt{PM}^{\text{nat}}$.

Without direct involvement of the PGD method, PM is continuous and path-independent, making it more reliable than LPS. In Figure 4, we depicted the box plot regarding PM for training data with various LPSs. The instability of LPS is evident: from the box centers, there is a little differentiation for data with large LPSs (e.g., LPS = 7 or 9) regarding PM; from the whiskers and outliers, the spreads of PMs are relatively scattered and the numbers of outliers are significant, confirming that the geometric messages characterized by LPS may not be very stable.

Algorithm 1 MAIL: The Overall Algorithm.

```
Input: a network model with the parameters $\theta$; and a training dataset $S$ of size $n$.
Output: a robust model with parameters $\theta^*$.
 1: for $e = 1$ to num_epoch do
 2:     for $b = 1$ to num_batch do
 3:         sample a mini-batch $\{(x_i, y_i)\}_{i=1}^m$ from $S$;          ▷ mini-batch of size $m$.
 4:         for $i = 1$ to batch_size do
 5:             $\delta_i^{(0)} = \xi$, with $\xi \sim \mathcal{U}(0,1)$;
 6:             for $t = 1$ to $T$ do
 7:                 $\delta_i^{(t)} \leftarrow \texttt{Proj}\left[\delta_i^{(t-1)} + \alpha\texttt{sign}\left(\nabla_\theta \ell(x_i + \delta_i^{(t-1)}, y_i; \theta)\right)\right]$;
 8:             end for
 9:             $w_i^{\text{unn}} = \texttt{sigmoid}(-\gamma(\texttt{PM}_i - \beta))$;
10:         end for
11:         $\omega_i = M \times w_i^{\text{unn}} / \sum_j w_j^{\text{unn}}, \forall i \in [m]$;          ▷ $\omega_i = 1$ during burn-in period.
12:         $\theta \leftarrow \theta - \eta \nabla_\theta \sum_{i=1}^m \omega_i \ell(x_i + \delta_i, y_i; \theta) + \mathcal{R}(x_i, y_i; \theta)$;
13:     end for
14: end for
```

3.2 Margin-Aware Instance Reweighting Learning (MAIL)

To benchmark our proposal against state-of-the-art counterparts, we propose the *margin-aware instance reweighting learning* (MAIL). The overall algorithm is summarized in Algorithm 1. Generally, the objective is $\sum_i \omega_i \ell(x_i + \delta_i^{(T)}, y_i; \theta) + \mathcal{R}(x_i, y_i; \theta)$, where $\mathcal{R}$ is an optional regularization term. This objective implies the optimization for the model, with one step (Step 5–8) generating the adversarial variants, one step (Step 9–11) calculating the importance weights, and one step (Step 12) minimizing the reweighted loss w.r.t. the model parameters.

Weight Assignment: We adopt the sigmoid function for weight assignment, which can be viewed as a *softened* sample selection operation of the form:

$$\omega_i^{\text{unn}} = \texttt{sigmoid}(-\gamma(\texttt{PM}_i - \beta)), \tag{8}$$

where β indicates how many data should have relatively large weights and $\gamma \geq 0$ controls the smoothness around β. Note that, $\texttt{PM}_i$ denotes the PM score for the i-th data point, which could be any one of $\texttt{PM}_i^{\text{adv}}$, $\texttt{PM}_i^{\text{nat}}$, and $\texttt{PM}_i^{\text{dif}}$. Eq. (8) is a monotonic function that assigns large values for data with small PMs, paying attention to critical data as discussed in Section 2.2. Moreover, it should be further normalized by $\omega_i = N \times w_i^{\text{unn}} / \sum_j w_j^{\text{unn}}$ to meet the constraint in Eq. (3).

Burn-in Period: During the initial training phase, the geometric information is less informative since the deep model is not adequately learned. Directly using the computed weights may mislead the training procedure and accumulate the bias in erroneous weight assignment. Therefore, we introduce a burn-in period at the beginning, where ω is fixed to 1 regardless of the corresponding PM value. A similar strategy has also been considered in Zhang et al. [47].

Two Realizations: The proposed MAIL is general for reweighting adversarial data, which can be combined with existing works. Here we give two representative examples: the first one is based on the vanilla AT [40], with the learning objective of the form (termed MAIL-AT):

$$-\sum_i \omega_i \log \mathbf{p}_{y_i}(x_i + \delta_i^{(T)}; \theta). \tag{9}$$

The second one is based on TRADES [45], which adopts the Kullback-Leibler (KL) divergence regarding natural and adversarial prediction, and also requires the learning guarantee (taken as a regularization term here) on the natural prediction. Overall, the learning objective is (termed MAIL-TRADES)

$$\beta \sum_i \omega_i \texttt{KL}(\mathbf{p}(x_i + \delta_i^{(T)}; \theta) || \mathbf{p}(x_i; \theta)) - \sum_i \log \mathbf{p}_{y_i}(x_i; \theta), \tag{10}$$

where $\beta > 0$ is the trade-off parameter and $\texttt{KL}(p||q) = \sum_k p_k \log p_k / q_k$ denotes the KL divergence.

Table 1: Comparison of LPS and PM on CIFAR-10 dataset.

	AT [29]			MART [40]			TRADES [45]		
	LPS	PM_{nat}	PM_{adv}	LPS	PM_{nat}	PM_{adv}	LPS	PM_{nat}	PM_{adv}
NAT	82.26 ± 0.60	82.50 ± 0.20	**83.15** ± **0.46**	**84.45** ± **0.17**	83.75 ± 0.09	84.12 ± 0.46	78.52 ± 0.20	**82.71** ± **0.52**	80.49 ± 0.18
PGD	54.14 ± 0.15	55.00 ± 0.32	**55.25** ± **0.23**	53.16 ± 0.26	53.63 ± 0.21	**53.65** ± **0.23**	51.67 ± 0.54	52.37 ± 0.65	**53.67** ± **0.14**
AA	36.32 ± 0.57	**44.25** ± **0.45**	44.10 ± 0.21	46.00 ± 0.26	46.70 ± 0.10	**47.20** ± **0.21**	44.40 ± 0.20	49.52 ± 0.11	**50.60** ± **0.22**

Our proposal is flexible and general enough in combining with many other advanced methods. For example, we can modify MART [40], which could discern correct/wrong prediction, to further utilize their geometric properties (termed MAIL-MART). Its formulation is similar to that of MAIL-TRADES with a slightly different learning objective, which is provided in Appendix C.

4 Experiments

We conducted extensive experiments on various datasets, including SVHN [32], CIFAR-10 [24], and CIFAR-100 [24]. The adopted backbone models are ResNet (ResNet-18) [21] and wide ResNet (WRN-32-10) [44]. In Section 4.2, we verified the effectiveness of PM as a geometric measurement. In Section 4.3, we benchmarked our MAIL against advanced methods. The source code of our paper can be found in github.com/QizhouWang/MAIL.

4.1 Experimental Setup

Training Parameters. For the considered methods, networks were trained using mini-batch gradient descent with momentum 0.9, weight decay 3.5×10^{-3} (for ResNet-18) / 7×10^{-4} (for WRN-32-10), batch size 128, and initial learning rate 0.01 (for ResNet-18) / 0.1 (for WRN-32-10) which is divided by 10 at the 75-th and 90-th epoch. To some extent, this setup can alleviate the impact of adversarial over-fitting [33, 40]. Moreover, following Madry et al. [29], the perturbation bound ϵ is $8/255$ and the (maximal) number of PGD steps k is 10 with step size $\alpha = 2/255$.

Hyperparameters. The slope and bias parameters were set to 10 and -0.5 in MAIL-AT and to 2 and 0 in both MAIL-TRADES and MAIL-MART. The trade-off parameter β was set to 5 in MAIL-TRADES, and to 6 in MAIL-MART (Algorithm 4 in Appendix C). For the training procedure, the weights started to update when the learning rate drop at the first time following Zhang et al. [47], i.e., the initial 74 epochs is burn-in period, and then we employed the reweighted objective functions.

Robustness Evaluation. We evaluated our methods and baselines using the standard accuracy on natural test data (NAT) and the adversarial robustness based on several attack methods, including the PGD method with 100 iterations [29], CW attack [8], APGD CE attack (APGD) [13], and auto attack (AA) [13]. All these methods have full access to the model parameters (i.e., *white-box* attacks) and are constrained by the same perturbation limit as above. Note that, here we do not focus on the *black-box* attack methods [4, 12, 26, 27, 48], which are relatively easy to be defensed [11].

4.2 Effectiveness of Probabilistic Margin

In this section, we verified the effectiveness of PM as a measurement in comparison with LPS. Here, we adopted ResNet-18 as the backbone model and conducted experiments on CIFAR-10 dataset.

Three basic methods were considered, including AT [29], MART [40], and TRADES [45], which were further assigned weights given by either PM or LPS [47]. For LPS, we adopted the assignment function in GAIRAT with the suggested setup [47]. We remind that AT-LPS, MART-LPS, and TRADES-LPS represent GAIRAT, GAIR-MART, and GAIR-TRADES in [47]; and AT-PM, MART-PM, and TRADES-PM represent MAIL-AT, MAIL-MART, and MAIL-TRADES, respectively. Note that, we validated two types of PM, namely, $\texttt{PM}^{\text{adv}}$ and $\texttt{PM}^{\text{nat}}$, which are very different from LPS.

Table 2: Average accuracy (%) and standard deviation on CIFAR-10 dataset with ResNet-18.

	NAT	PGD	APGD	CW	AA
AT [29]	84.86 ± 0.17	48.91 ± 0.14	47.70 ± 0.06	51.61 ± 0.15	44.90 ± 0.53
TRADES [45]	84.00 ± 0.23	52.66 ± 0.16	52.37 ± 0.24	52.30 ± 0.06	48.10 ± 0.26
MART [40]	82.28 ± 0.14	53.50 ± 0.46	52.73 ± 0.57	51.59 ± 0.16	48.40 ± 0.14
FAT [46]	**87.97** ± **0.15**	46.78 ± 0.12	46.68 ± 0.16	49.92 ± 0.26	43.90 ± 0.82
AWP [42]	85.17 ± 0.40	52.63 ± 0.17	50.40 ± 0.26	51.39 ± 0.18	47.00 ± 0.25
GAIRAT [47]	83.22 ± 0.06	54.81 ± 0.15	50.95 ± 0.49	39.86 ± 0.08	33.35 ± 0.57
MAIL-AT	84.52 ± 0.46	**55.25** ± **0.23**	**53.20** ± **0.38**	48.88 ± 0.11	44.22 ± 0.21
MAIL-TRADES	81.84 ± 0.18	53.68 ± 0.14	52.92 ± 0.62	**52.89** ± **0.31**	**50.60** ± **0.22**

The experimental results with 5 individual trials are summarized in Table 1, where we adopted three evaluations, including natural performance (NAT), the PGD method with 100 steps (PGD), and auto attack (AA). AA can be viewed as an ensemble of several advanced attacks and thus reliably reflect the robustness. As we can see, the superiority of PM is apparent, regardless of the adopted learning objectives: the results of PM are 0.70-7.93% better than LPS regarding AA and 0.14-2.00% better regarding PGD. Although LPS could achieve comparable results regarding PGD attacks, its adversarial robustness is quite low when facing AA attacks. It indicates that the robustness improvement of GAIRAT might be partially. This is probably caused by *obfuscated gradients* [2], since stronger attack methods (e.g., AA) lead to poorer performance on adversarial robustness.

Comparing the results in using PM_{nat} and PM_{adv}, both PMs can lead to promising robustness, while PM_{adv} is slightly better. The reason is that PM_{adv} can precisely describe the distance between adversarial variants and decision boundaries. As a result, it can help accurately assign high wights for those important instances during AT. Therefore, we adopt PM_{adv} in the following experiments.

4.3 Performance Evaluation

We also benchmarked our proposal against advanced methods. Here, we reported the results on the CIFAR-10 dataset due to the space limitation. Please refer to Appendix B for more results.

Compared Baselines. We compared the proposed method with the following baselines: (1) (traditional) AT [29]: the cross-entropy loss for adversarial perturbation generated by the PGD method; (2) TRADES [45]: a learning objective with an explicit trade-off between the adversarial and natural performance; (3) MART [40]: a training strategy which treats wrongly/correctly predicted data separately; (4) FAT [46]: adversarial training with early-stopping in adversarial intensity; (5) AWP [42]: a double perturbation mechanism that can flatten the loss landscape by weight perturbation; (6) GAIRAT [47]: geometric-aware instance-reweighted adversarial training.

All the methods were run for 5 individual trials with different random seeds, where we reported their average accuracy and standard deviation. The results are summarized in Table 2 and Table 3 with the backbone models being ResNet-18 and WRN-32-10, respectively. Overall, our MAIL achieved the best or the second-best robustness against all four types of attacks, revealing the superiority of MAIL (i.e., MAIL-AT and MAIL-TRADES) in adversarial robustness. Specifically, AT and TRADES both treat training data equally, and thus their results were unsatisfactory compared with the best one ($0.55\% - 6.34\%$ decline with ResNet-18 and $0.02\% - 9.43\%$ decline with WRN-32-10), implying the possibility for its further improvement. Though MART and FAT consider the impact

Table 3: Average accuracy (%) and standard deviation on CIFAR-10 dataset with WRN-32-10.

	NAT	PGD	APGD	CW	AA
AT	87.80 ± 0.13	49.43 ± 0.29	49.12 ± 0.26	53.38 ± 0.05	48.46 ± 0.46
TRADES	86.36 ± 0.52	54.88 ± 0.39	55.02 ± 0.27	56.18 ± 0.16	53.40 ± 0.37
‘ MART	84.76 ± 0.34	55.61 ± 0.51	55.40 ± 0.37	54.72 ± 0.20	51.40 ± 0.05
FAT	**89.70** ± **0.17**	48.79 ± 0.18	48.72 ± 0.36	52.39 ± 0.89	47.48 ± 0.30
AWP	57.55 ± 0.23	54.17 ± 0.10	54.20 ± 0.16	55.18 ± 0.30	53.08 ± 0.17
GAIRAT	86.30 ± 0.61	58.74 ± 0.46	55.64 ± 0.36	45.57 ± 0.18	40.30 ± 0.16
MAIL-AT	84.83 ± 0.39	**58.86** ± **0.25**	55.82 ± 0.31	51.26 ± 0.20	47.10 ± 0.22
MAIL-TRADES	84.00 ± 0.15	57.40 ± 0.96	**56.96** ± **0.19**	**56.20** ± **0.30**	**53.90** ± **0.22**

of individuals on the final performance, they fail in paying attention to geometric properties of data during training. Concretely, MART mainly focuses on the correctness regarding natural prediction, and FAT prevents the model learning from *highly* non-robust data in keeping its natural performance. Therefore, FAT achieved the best natural performance ($3.11\% - 6.13\%$ improvement with ResNet-18 and $1.90\% - 5.70\%$ improvement with WRN-32-10), while its robustness against adversaries seems inadequate ($2.97\% - 8.45\%$ decline with ResNet-18 and 3.81%-10.07% decline with WRN-32-10). Moreover, in adopting LPS as the geometric measurement, GAIRAT performed well regarding PGD and AGPD attacks, while the adversarial robustness on CW and AA attacks were pretty low. In comparison, we retained the supremacy on PGD-based attacks (i.e., PGD and APGD) as in GAIRAT and revealed promising results regarding CW and AA attacks. For example, in Table 2, we achieved 0.44%-8.47% improvements on PGD attack, 0.47%-6.52% on APGD attack, 0.59%-13.03% on CW attack, and 1.63%-16.68% on AA attack.

MAIL-AT performed well on PGD-based methods, while MAIL-TRADES was good at CW and AA attacks. It suggests that the robustness depends on adopted learning objectives, coinciding with the previous conclusion [40]. In general, we suggest using MAIL-TRADES as a default choice, as it reveals promising results regarding AA while keeping a relatively high performance regarding PGD-based attacks. Besides, comparing the results in Table 2 and Table 3, the overall accuracy had a promising improvement in employing models with a much large capacity (i.e., WRN-32-10), verifying the fact that deep models have insufficient network capacity in fitting adversaries [47].

5 Conclusion

In this paper, we focus on boosting adversarial robustness by reweighting adversarial data during training, where data closer to the current decision boundaries are more critical and thus require larger weights. To measure the closeness, we suggest the use of *probabilistic margin* (PM), which relates to the multi-class margin in the probability space of model outputs (i.e., the estimated class-posterior probabilities). Without any involvement of the PGD iterations, PM is continuous and path-independent and thus overcomes the drawbacks of previous works (e.g., LPS) efficaciously. Moreover, we consider several types of PMs with different geometric properties, and propose a general framework termed MAIL. Experiments demonstrated that PMs are more reliable measurements than previous works, and our MAIL revealed its superiority against state-of-the-art methods, independent of adopted (basic) learning objectives. In the future, we will delve deep into the mechanism in instance-reweighted adversarial learning, theoretically study the contribution of individuals for the final performance, and improve the methodology in using geometric characteristics of data.

Acknowledgments and Disclosure of Funding

QZW and BH were supported by the RGC Early Career Scheme No. 22200720, NSFC Young Scientists Fund No. 62006202 and HKBU CSD Departmental Incentive Grant. TLL was partially supported by Australian Research Council Projects DP-180103424, DE-190101473, and IC-190100031. GN and MS were supported by JST AIP Acceleration Research Grant Number JPMJCR20U3, Japan, and MS was also supported by Institute for AI and Beyond, UTokyo.

References

[1] M. Andriushchenko and N. Flammarion. Understanding and improving fast adversarial training. In *NeurIPS*, 2020.

[2] A. Athalye, N. Carlini, and D. A. Wagner. Obfuscated gradients give a false sense of security: Circumventing defenses to adversarial examples. In *ICML*, 2018.

[3] A. Athalye, L. Engstrom, A. Ilyas, and K. Kwok. Synthesizing robust adversarial examples. In *ICML*, 2018.

[4] Y. Bai, Y. Zeng, Y. Jiang, Y. Wang, S. Xia, and W. Guo. Improving query efficiency of black-box adversarial attack. In *ECCV*, 2020.

[5] M. Balunovic and M. Vechev. Adversarial training and provable defenses: Bridging the gap. In *ICLR*, 2019.

[6] A. N. Bhagoji, W. He, B. Li, and D. Song. Practical black-box attacks on deep neural networks using efficient query mechanisms. In *ECCV*, 2018.

[7] S. Bubeck, Y. T. Lee, E. Price, and I. P. Razenshteyn. Adversarial examples from computational constraints. In *ICML*, 2019.

[8] N. Carlini, A. Athalye, N. Papernot, W. Brendel, J. Rauber, D. Tsipras, I. Goodfellow, A. Madry, and A. Kurakin. On evaluating adversarial robustness. *arXiv preprint arXiv:1902.06705*, 2019.

[9] N. Carlini and D. A. Wagner. Towards evaluating the robustness of neural networks. In *Proceedings of the 2017 IEEE Symposium on Security and Privacy*, 2017.

[10] Y. Carmon, A. Raghunathan, L. Schmidt, P. Liang, and J. C. Duchi. Unlabeled data improves adversarial robustness. In *NeurIPS*, 2019.

[11] A. Chakraborty, M. Alam, V. Dey, A. Chattopadhyay, and D. Mukhopadhyay. A survey on adversarial attacks and defences. *CAAI Transactions on Intelligence Technology*, 6:25–45, 2021.

[12] M. Cheng, T. Le, P. Chen, H. Zhang, J. Yi, and C. Hsieh. Query-efficient hard-label black-box attack: An optimization-based approach. In *ICLR*, 2019.

[13] F. Croce and M. Hein. Reliable evaluation of adversarial robustness with an ensemble of diverse parameter-free attacks. In *ICML*, 2020.

[14] D. Cullina, A. N. Bhagoji, and P. Mittal. Pac-learning in the presence of evasion adversaries. In *NeurIPS*, 2018.

[15] J. Dong, Y. Cong, G. Sun, and D. Hou. Semantic-transferable weakly-supervised endoscopic lesions segmentation. In *ICCV*, 2019.

[16] J. Dong, Y. Cong, G. Sun, B. Zhong, and X. Xu. What can be transferred: Unsupervised domain adaptation for endoscopic lesions segmentation. In *CVPR*, 2020.

[17] X. Du, J. Zhang, B. Han, T. Liu, Y. Rong, G. Niu, J. Huang, and M. Sugiyama. Learning diverse-structured networks for adversarial robustness. In *ICML*, 2021.

[18] A. Fawzi, S. Moosavi-Dezfooli, P. Frossard, and S. Soatto. Empirical study of the topology and geometry of deep networks. In *CVPR*, 2018.

[19] S. G. Finlayson, J. D. Bowers, J. Ito, J. L. Zittrain, A. L. Beam, and I. S. Kohane. Adversarial attacks on medical machine learning. *Science*, 363(6433):1287–1289, 2019.

[20] R. Gao, F. Liu, J. Zhang, B. Han, T. Liu, G. Niu, and M. Sugiyama. Maximum mean discrepancy test is aware of adversarial attacks. In *ICML*, 2021.

[21] K. He, X. Zhang, S. Ren, and J. Sun. Deep residual learning for image recognition. In *CVPR*, 2016.

[22] A. Ilyas, S. Santurkar, D. Tsipras, L. Engstrom, B. Tran, and A. Madry. Adversarial examples are not bugs, they are features. In *NeurIPS*, 2019.

[23] V. Koltchinskii and D. Panchenko. Empirical margin distributions and bounding the generalization error of combined classifiers. *Annals of Statistics*, 30(1):1–50, 2002.

[24] A. Krizhevsky and G. Hinton. Learning multiple layers of features from tiny images. *Technical Report TR-2009, University of Toronto, Toronto*, 2009.

[25] A. Kurakin, I. J. Goodfellow, and S. Bengio. Adversarial examples in the physical world. In *ICLR*, 2017.

[26] J. Li, R. Ji, H. Liu, J. Liu, B. Zhong, C. Deng, and Q. Tian. Projection & probability-driven black-box attack. In *CVPR*, 2020.

[27] Y. Li, L. Li, L. Wang, T. Zhang, and B. Gong. NATTACK: learning the distributions of adversarial examples for an improved black-box attack on deep neural networks. In *ICML*, 2019.

[28] G. Litjens, T. Kooi, B. E. Bejnordi, A. A. A. Setio, F. Ciompi, M. Ghafoorian, J. A. Van Der Laak, B. Van Ginneken, and C. I. Sánchez. A survey on deep learning in medical image analysis. *Medical Image Analysis*, 42:60–88, 2017.

[29] A. Madry, A. Makelov, L. Schmidt, D. Tsipras, and A. Vladu. Towards deep learning models resistant to adversarial attacks. In *ICLR*, 2018.

[30] S.-M. Moosavi-Dezfooli, A. Fawzi, J. Uesato, and P. Frossard. Robustness via curvature regularization, and vice versa. In *CVPR*, 2019.

[31] Y. Nesterov. A method for solving the convex programming problem with convergence rate O(1/kˆ2). *Proceedings of the USSR Academy of Sciences*, 269:543–547, 1983.

[32] Y. Netzer, T. Wang, A. Coates, A. Bissacco, B. Wu, and A. Y. Ng. Reading digits in natural images with unsupervised feature learning. In *NeurIPS Workshop on Deep Learning and Unsupervised Feature Learning*, 2011.

[33] T. Pang, X. Yang, Y. Dong, H. Su, and J. Zhu. Bag of tricks for adversarial training. In *ICLR*, 2021.

[34] N. Papernot, P. McDaniel, A. Sinha, and M. Wellman. Towards the science of security and privacy in machine learning. In *Proceedings of 3rd IEEE European Symposium on Security and Privacy*, 2018.

[35] Y. Qin, N. Carlini, G. W. Cottrell, I. J. Goodfellow, and C. Raffel. Imperceptible, robust, and targeted adversarial examples for automatic speech recognition. In *ICML*, 2019.

[36] L. Schmidt, S. Santurkar, D. Tsipras, K. Talwar, and A. Madry. Adversarially robust generalization requires more data. In *NeurIPS*, 2018.

[37] C. Szegedy, W. Zaremba, I. Sutskever, J. Bruna, D. Erhan, I. J. Goodfellow, and R. Fergus. Intriguing properties of neural networks. In *ICLR*, 2014.

[38] D. Tsipras, S. Santurkar, L. Engstrom, A. Turner, and A. Madry. Robustness may be at odds with accuracy. In *ICLR*, 2019.

[39] H. Wang, T. Chen, S. Gui, T.-K. Hu, J. Liu, and Z. Wang. Once-for-all adversarial training: In-situ tradeoff between robustness and accuracy for free. In *NeurIPS*, 2020.

[40] Y. Wang, D. Zou, J. Yi, J. Bailey, X. Ma, and Q. Gu. Improving adversarial robustness requires revisiting misclassified examples. In *ICLR*, 2020.

[41] E. Wong, L. Rice, and J. Z. Kolter. Fast is better than free: Revisiting adversarial training. In *ICLR*, 2020.

[42] D. Wu, S.-T. Xia, and Y. Wang. Adversarial weight perturbation helps robust generalization. In *NeurIPS*, 2020.

[43] X. Yu, G. Chen, and S. Cheng. Dynamic learning rate optimization of the backpropagation algorithm. *IEEE Transactions on Neural Networks*, 6(3):669–677, 1995.

[44] S. Zagoruyko and N. Komodakis. Wide residual networks. In *BMVC*, 2016.

[45] H. Zhang, Y. Yu, J. Jiao, E. P. Xing, L. E. Ghaoui, and M. I. Jordan. Theoretically principled trade-off between robustness and accuracy. In *ICML*, 2019.

[46] J. Zhang, X. Xu, B. Han, G. Niu, L. Cui, M. Sugiyama, and M. S. Kankanhalli. Attacks which do not kill training make adversarial learning stronger. In *ICML*, 2020.

[47] J. Zhang, J. Zhu, G. Niu, B. Han, M. Sugiyama, and M. Kankanhalli. Geometry-aware instance-reweighted adversarial training. In *ICLR*, 2021.

[48] Y. Zhang, Y. Li, T. Liu, and X. Tian. Dual-path distillation: A unified framework to improve black-box attacks. In *ICML*, 2020.

[49] D. Zhou, T. Liu, B. Han, N. Wang, C. Peng, and X. Gao. Towards defending against adversarial examples via attack-invariant features. In *ICML*, 2021.

A Line-Search & Momentum-PGD (LM-PGD)

Here, we describe the detailed realization of the Line-Search & Momentum-PGD (LM-PGD) method. Compared with the commonly used PGD method of the form following

$$\delta_i^{(t)} \leftarrow \texttt{Proj}\left[\delta_i^{(t-1)} + \alpha\texttt{sign}\left(\nabla_\theta \ell(x_i + \delta_i^{(t-1)}, y_i; \theta)\right)\right], \tag{11}$$

the Line-Search & Momentum-PGD makes two improvements: (1) we use the Nesterov gradient [31] in an attempt to overcome the sub-optimal points, i.e.,

$$v_i^{(t)} \leftarrow \gamma v_i^{(t-1)} + \alpha^{(t-1)}\texttt{sign}\left(\nabla_\theta \ell(x_i + \delta_i^{(t-1)}, y_i; \theta)\right), \tag{12}$$

$$\delta_i^{(t)} \leftarrow \texttt{Proj}\left[\delta_i^{(t-1)} + v_i^{(t)}\right], \tag{13}$$

where γ is the momentum parameter and $\alpha^{(t)}$ is the step size at the t-th iteration; (2) and we adopt the line-searched step size [43], which aims at finding the optimal $\alpha^{(t-1)}$ in a predefined searching space $V = [\alpha^{(\text{min})}, \alpha^{(\text{max})}]$, namely

$$\alpha^{(t-1)} \leftarrow \arg\max_{\alpha \in V} \ell\left(x_i + \texttt{Proj}\left[\delta_i^{(t-1)} + \gamma v_i^{(t-1)} + \alpha\texttt{sign}\left(\nabla_\theta \ell(x_i + \delta_i^{(t-1)}, y_i; \theta)\right)\right], y_i; \theta\right). \tag{14}$$

In Figure 1(a), the maximal PGD iteration is 50, with γ being 0.8, $\alpha^{(\text{max})}$ being $6/255$, and $\alpha^{(\text{min})}$ being $4/255$ in the first 15 iterations and 0 otherwise.

Note that, the LM-PGD cannot remove the drawbacks of the LPS with the following reasons: (1) the path-dependency property exists as the LM-PGD still uses the first-order gradients for optimization; (2) the momentum term and the line-searched learning rate would make the corresponding LPS difficult to be computed since each step may have different length. As the LM-PGD cannot be directly used in assigning weights, we proposed the PM in this paper.

B Further Experiments

To further demonstrate the robustness of our proposal against adversarial attacks, we also conducted experiments on SVHN [32] and CIFAR-100 [32] datasets. Here we adopted ResNet-18 as the backbone model with the same experimental setup as in Section 4.2, where we reported the natural accuracy (NAT), PGD-100 attack (PGD), and auto-attack (AA). All the experiments are conducted for 5 individual trails, and the average performance and standard deviations are summarized in Table 4. Note that, all the methods were realized by Pytorch 1.81 [3] with CUDA 11.1 [4], where we used several GeForce RTX 3090 GPUs and AMD Ryzen Threadripper $3960X$ Processors.

Some advanced methods (e.g., TRADES and MART) can hardly beat the traditional AT on these two datasets, indicating the performance of the learning methods may also depend on the considered datasets. Moreover, FAT retains the highest natural performance (i.e., NAT) but its results on PGD and AA are relatively low, which are similar to Table 2 and Table 3. For GAIRAT on CIFAR-100, we observe that its performance on the PGD attack was not as high as some other datasets (e.g., SVHN and CIFAR-10), it may reveal that the deficiencies of LPS are non-negligible for some difficult tasks. There may exist some better reweighting strategies in boosting adversarial robustness. As we can see, our MAIL-AT and MAIL-TRADES, which benefit from the proposed PM, achieved the best or the comparable (e.g., AA on CIFAR-100) performance regarding various adversarial attacks, and the natural accuracy retained to be acceptable.

Further, we tested the effectiveness in adopting the probabilistic space, where we compare our PM with the results given by multi-class margin (denoted by MM) of the form:

$$f_{y_i}(x_i;\theta) - \max_{j, j\neq y_i} f_j(x_i;\theta), \tag{15}$$

where f denotes the model outputs before the softmax link function and f_j denotes its j-th dimensional value. We conducted experiments on CIFAR-10 dataset with the backbone being ResNet-18

[3] https://pytorch.org/

[4] https://developer.nvidia.com/

Table 4: Average test accuracy (%) and standard deviation (5 trials) on SVHN and CIFAR-100.

		SVHN			CIFAR-100	
	NAT	PGD	AA	NAT	PGD	AA
AT	93.55 ± 0.65	54.76 ± 0.30	46.58 ± 0.46	60.13 ± 0.39	28.69 ± 0.24	24.76 ± 0.25
TRADES	93.65 ± 0.29	55.12 ± 0.68	45.74 ± 0.31	60.73 ± 0.33	29.83 ± 0.25	24.90 ± 0.33
MART	92.57 ± 0.14	55.45 ± 0.26	43.52 ± 0.43	54.08 ± 0.60	29.94 ± 0.21	**25.30 ± 0.50**
FAT	**93.68 ± 0.31**	53.81 ± 0.77	41.68 ± 0.49	**66.74 ± 0.28**	23.25 ± 0.55	20.88 ± 0.13
AWP	93.34 ± 0.22	57.62 ± 0.31	47.21 ± 0.30	55.16 ± 0.27	30.14 ± 0.30	25.16 ± 0.39
GAIRAT	90.47 ± 0.77	64.67 ± 0.26	37.00 ± 0.30	58.43 ± 0.28	25.74 ± 0.51	17.54 ± 0.33
MAIL-AT	**93.68 ± 0.25**	**65.54 ± 0.16**	41.12 ± 0.30	60.74 ± 0.15	27.62 ± 0.27	22.44 ± 0.53
MAIL-TRADES	89.68 ± 0.19	58.40 ± 0.21	**49.10 ± 0.22**	60.13 ± 0.25	**30.28 ± 0.19**	24.80 ± 0.25

Table 5: Comparison of MM and PM on CIFAR-10 dataset with average test accuracy (%) and standard deviation (5 trails).

	MM	PM
NAT	80.44 ± 0.21	**81.84 ± 0.18**
PGD	53.58 ± 0.11	**53.68 ± 0.14**
AA	49.20 ± 0.09	**50.60 ± 0.22**

Table 6: Comparison with different weight assignment functions on CIFAR-10 dataset with average test accuracy (%) and standard deviation (5 trails).

	hinge	step	sigmoid
NAT	80.17 ± 0.17	81.11 ± 0.15	**81.84 ± 0.18**
PGD	52.23 ± 0.31	53.53 ± 0.14	**53.68 ± 0.14**
AA	43.40 ± 0.22	50.30 ± 0.20	**50.60 ± 0.22**

and the basic method being TRADES. The experimental results are listed in the Table 5. As we can see, the normalized embedding features (i.e., our PM) would genuinely lead to better results regarding both natural accuracy (NAT) and adversarial robustness (PGD and AA), verifying the effectiveness in using the probabilistic margin (instead of the commonly-used multi-class margin) as the measurement for geometry-aware adversarial training.

Now, we made investigations of the formulations in assigning weights. In Table 6, we further adopted the following two assignment functions, namely, the hinge-shaped function $\max(0, \gamma(\mathtt{PM}_i - \beta))$ and the step function $\begin{cases} \alpha & \text{if } \mathtt{PM}_i > \beta \\ 1-\alpha & \text{if } \mathtt{PM}_i \leq \beta \end{cases}$ (with $\alpha = 0.2$). We conducted experiments on CIFAR-10 dataset with backbone being ResNet-18 and basic method being TRADES. The results are listed in Table 6. As we can see, compared with these commonly-used assignment functions, the sigmoid function can truly achieve superior performance, coincide with previous observation in [47]. The reason is that, the sigmoid-shaped functions are strictly monotonic and continuous, where the resulting weights can retain the underlying geometric properties of data properly. In comparison, the robustness regarding AA attack given by hinge-shaped function is far below other assignment functions, since it ignore all those data with $\mathtt{PM}_i - \beta < 0$ by assigning weights with value being 0. Further, the results given by the step function is also lower than our sigmoid-shaped function, since it can not distinguish data with different geometric properties if all these data are greater/smaller than β.

In the end, it is also interesting in adopting other attacks methods in our learning framework, to demonstrate that our proposal is general to most of the attack methods. Here, we adopted PGD (as used in AT), CW, and KL (as used in TRADES) in generating adversarial perturbations, and we used the learning objectives given by AT and TRADES. We conducted experiments on CIFAR-10 dataset with ResNet-18, and the results are listed in Table 7. In general, adopting the KL method would

Table 7: MAIL with different methods in generating adversarial perturbations on CIFAR-10 dataset.

	AT			TRADES		
	NAT	PGD	AA	NAT	PGD	AA
PGD	84.52 ± 0.46	55.25 ± 0.23	**44.22 ± 0.21**	80.83 ± 0.31	54.84 ± 0.15	49.90 ± 0.10
CW	81.84 ± 0.25	**65.55 ± 0.20**	37.20 ± 0.18	80.33 ± 0.19	**57.55 ± 0.32**	50.20 ± 0.25
KL	**85.33 ± 0.30**	51.34 ± 0.14	32.10 ± 0.22	**81.84 ± 0.18**	53.68 ± 0.14	**50.60 ± 0.22**

lead to better results on natural accuracy, while adversarial robustness regarding the PGD attack prefers to learn from the perturbation generated by CW. It coincides with the previous conclusion that adversarial training is not adaptive [34]. Further, for the AA attack, TRADES revealed much stable and superior results regarding various methods in generating perturbations, compared with the results given by AT.

C Realizations of MAIL

Here, we provide the detailed algorithms for our three realizations, namely, MAIL-AT (in Algorithm 2), MAIL-TRADES (in Algorithm 3), and MAIL-MART (in Algorithm 4). In Algorithm 4, the *boosted cross entropy* (BCE) loss is of the form:

$$\texttt{BCE}(x_i + \delta_i^{(T)}, y_i; \theta) = -\log \mathbf{p}_{y_i}(x_i + \delta_i^{(T)}) - \log(1 - \max_{k \neq y_i} \mathbf{p}_k(x_i + \delta_i^{(T)})), \tag{16}$$

where the first term in the r.h.s. is the common cross entropy loss and the second term is a regularization term that that make the prediction much confident. The *mis-classification aware KL* (MKL) term is of the form:

$$\texttt{MKL}(x_i, \delta_i^{(T)}; \theta) = \texttt{KL}(\mathbf{p}(x_i + \delta_i^{(T)}; \theta) || \mathbf{p}(x_i; \theta))(1 - \mathbf{p}_{y_i}(x_i; \theta)), \tag{17}$$

which reweights the KL-divergence by the estimated probability of a correct prediction.

D Further Discussion

We adopt an instance-reweighting learning framework and propose PMs in measuring the robustness regarding adversarial attacks. Our PMs are continuous and path-independent, overcoming the deficiency of previous works [47]. The overall method is general and flexible, combined with existing works to boost their primary performance.

Moreover, there is still room for improvement in our approach and related works. This paper mainly focuses on adversarial robustness regarding white-box attacks generated by the first-order gradient-based methods. When employing our MAIL in real-world applications, it may lead to over-confidence regarding many other attacks, e.g., provable attacks [5], black-box attacks [6], and physical attacks [25]. It poses the potential risk and dangers for the resulting systems (e.g., autonomous driving), as it would produce non-robust behavior unexpectedly when encountering unseen types of attacks.

The problems of fairness should also be considered since individuals are not treated equally during training. For data assigned with larger weights, the resulting model would be more robust when encounters similar data during the test. This unfairness problem seems inevitable for a reweighted learning framework, which will interest our further study. Moreover, our method might be more vulnerable to error-prone data (e.g., with label noise) than traditional AT since MAIL would provide abnormal weights (e.g., larger weights than expectation) for these data. This issue would mislead the training procedure in fitting *noise*, which has an apparent negative impact on the model.

Algorithm 2 MAIL-AT: The Overall Algorithm.

```
Input: a network model with the parameters $\theta$; and a training dataset $S$ of size $n$.
Output: a robust model with parameters $\theta^*$.
for $e = 1$ to num_epoch do
    for $b = 1$ to num_batch do
        sample a mini-batch $\{(x_i, y_i)\}_{i=1}^m$ from $S$;        ▷ mini-batch of size $m$.
        for $i = 1$ to batch_size do
            $\delta_i^{(0)} = \xi$, with $\xi \sim \mathcal{U}(0, 1)$;
            for $t = 1$ to $T$ do
                $\delta_i^{(t)} \leftarrow \texttt{Proj}\left[\delta_i^{(t-1)} + \alpha\texttt{sign}\left(\nabla_\theta - \log \mathbf{p}_{y_i}(x_i + \delta_i^{(t-1)}; \theta)\right)\right]$;
            end for
            $w_i^{\text{unn}} = \texttt{sigmoid}(-\gamma(\texttt{PM}_i - \beta))$;
        end for
        $\omega_i = M \times w_i^{\text{unn}} / \sum_j w_j^{\text{unn}}, \forall i \in [m]$;        ▷ $\omega_i = 1$ during burn-in period.
        $\theta \leftarrow \theta - \eta\nabla_\theta\left(-\sum_{i=1}^m \omega_i \log \mathbf{p}_{y_i}(x_i + \delta_i^{(T)}; \theta)\right)$;
    end for
end for
```

Algorithm 3 MAIL-TRADES: The Overall Algorithm.

```
Input: a network model with the parameters $\theta$; and a training dataset $S$ of size $n$.
Output: a robust model with parameters $\theta^*$.
for $e = 1$ to num_epoch do
    for $b = 1$ to num_batch do
        sample a mini-batch $\{(x_i, y_i)\}_{i=1}^m$ from $S$;        ▷ mini-batch of size $m$.
        for $i = 1$ to batch_size do
            $\delta_i^{(0)} = \xi$, with $\xi \sim \mathcal{U}(0, 1)$;
            for $t = 1$ to $T$ do
                $\delta_i^{(t)} \leftarrow \texttt{Proj}\left[\delta_i^{(t-1)} + \alpha\texttt{sign}\left(\nabla_\theta\texttt{KL}(\mathbf{p}(x_i + \delta_i^{(t-1)}; \theta) || \mathbf{p}(x_i; \theta))\right)\right]$;
            end for
            $w_i^{\text{unn}} = \texttt{sigmoid}(-\gamma(\texttt{PM}_i - \beta))$;
        end for
        $\omega_i = M \times w_i^{\text{unn}} / \sum_j w_j^{\text{unn}}, \forall i \in [m]$;        ▷ $\omega_i = 1$ during burn-in period.
        $\theta \leftarrow \theta - \eta\nabla_\theta \sum_i \left(\beta\omega_i\texttt{KL}(\mathbf{p}(x_i + \delta_i^{(T)}; \theta) || \mathbf{p}(x_i; \theta)) - \sum_i \log \mathbf{p}_{y_i}(x_i; \theta)\right)$;
    end for
end for
```

Algorithm 4 MAIL-MART: The Overall Algorithm.

```
Input: a network model with the parameters $\theta$; and a training dataset $S$ of size $n$.
Output: a robust model with parameters $\theta^*$.
for $e = 1$ to num_epoch do
    for $b = 1$ to num_batch do
        sample a mini-batch $\{(x_i, y_i)\}_{i=1}^m$ from $S$;        ▷ mini-batch of size $m$.
        for $i = 1$ to batch_size do
            $\delta_i^{(0)} = \xi$, with $\xi \sim \mathcal{U}(0, 1)$;
            for $t = 1$ to $T$ do
                $\delta_i^{(t)} \leftarrow \texttt{Proj}\left[\delta_i^{(t-1)} + \alpha\texttt{sign}\left(\nabla_\theta - \log \mathbf{p}_{y_i}(x_i + \delta_i^{(t-1)}; \theta)\right)\right]$;
            end for
            $w_i^{\text{unn}} = \texttt{sigmoid}(-\gamma(\texttt{PM}_i - \beta))$;
        end for
        $\omega_i = M \times w_i^{\text{unn}} / \sum_j w_j^{\text{unn}}, \forall i \in [m]$;        ▷ $\omega_i = 1$ during burn-in period.
        $\theta \leftarrow \theta - \eta\nabla_\theta\left(-\sum_{i=1}^m \omega_i\texttt{BCE}(x_i + \delta_i^{(T)}, y_i; \theta) + \beta\texttt{MKL}(x_i, \delta_i^{(T)}; \theta)\right)$;
    end for
end for
```

Checklist

1. For all authors...
   (a) Do the main claims made in the abstract and introduction accurately reflect the paper's contributions and scope? [Yes]
   (b) Did you describe the limitations of your work? [Yes] We have discussed the potential drawbacks of our proposal in Appendix B.
   (c) Did you discuss any potential negative societal impacts of your work? [Yes]
   (d) Have you read the ethics review guidelines and ensured that your paper conforms to them? [Yes]
2. If you are including theoretical results...
   (a) Did you state the full set of assumptions of all theoretical results? [N/A]
   (b) Did you include complete proofs of all theoretical results? [N/A]
3. If you ran experiments...
   (a) Did you include the code, data, and instructions needed to reproduce the main experimental results (either in the supplemental material or as a URL)? [Yes]
   (b) Did you specify all the training details (e.g., data splits, hyperparameters, how they were chosen)? [Yes]
   (c) Did you report error bars (e.g., with respect to the random seed after running experiments multiple times)? [Yes]
   (d) Did you include the total amount of compute and the type of resources used (e.g., type of GPUs, internal cluster, or cloud provider)? [Yes] We have discussed the computing resources in Appendix B.
4. If you are using existing assets (e.g., code, data, models) or curating/releasing new assets...
   (a) If your work uses existing assets, did you cite the creators? [N/A]
   (b) Did you mention the license of the assets? [N/A]
   (c) Did you include any new assets either in the supplemental material or as a URL? [No]
   (d) Did you discuss whether and how consent was obtained from people whose data you're using/curating? [No] We use only standard datasets
   (e) Did you discuss whether the data you are using/curating contains personally identifiable information or offensive content? [No] We use only standard datasets
5. If you used crowdsourcing or conducted research with human subjects...
   (a) Did you include the full text of instructions given to participants and screenshots, if applicable? [N/A]
   (b) Did you describe any potential participant risks, with links to Institutional Review Board (IRB) approvals, if applicable? [N/A]
   (c) Did you include the estimated hourly wage paid to participants and the total amount spent on participant compensation? [N/A]